AIR FORCED CONVECTION OVER A TWO-SIDED PLATE EXTENDED BY RECTANGULAR HOLLOW BLOCKS

by

Vadim DUBOVSKY * ***and Ruth LETAN***

Heat Transfer Laboratory, Department of Mechanical Engineering,
Ben-Gurion University of the Negev, Beer-Sheva, Israel

Original scientific paper
https://doi.org/10.2298/TSCI19S4251D

Our work focuses on an array of hollow blocks formed on a two-sided plate, inserted in a rectangular channel, heated and exposed to forced convection of air at room temperature. The thermal performance of the extended surface of the plates is investigated within a range of air velocities and power input. The investigation is conducted experimentally, using an infrared camera, and numerically in a 3-D computational domain.

The experimental results and the numerical calculations showed quantitatively a satisfactory agreement. As expected, the heat transfer rates significantly increased as the air velocity in the channel increased. At low velocities the thermal performance of the extended plate compared to the performance of a flat plate.

A numerical analysis of the extensions size and the ratio of plate height to width were also carried out and its effect upon the thermal performance of the system was examined. Relation between fluid pressure losses and heat transfer was studied and generalized.

The application of the surfaces extended by blocks is found in several industries, for example in electronic equipment, solar industry, and others.

Keywords: *extended surface*, *rectangular blocks*, *forced convection, numeric analysis, correlations, infrared visualization*

Introduction

The use of extended surfaces has two main goals. Firstly, they are used to intensify the heat transfer on the air side of heat transfer surfaces. Further, in cases where the heat sources themselves have a block structure, which is also characteristic in engineering applications, as cooling of electronic systems.

Sparrow *et al.* [1] presented an experiment on heat transfer and pressure drop for airflow in arrays of heat generating modules deployed along one wall of a flat rectangular duct. The effects of missing elements, height difference between modules and implanted barriers were investigated. Chang and You [2] investigated the heat transfer from two hot blocks to mixed convective flow in a channel. The components are not mounted on the plates or boards, thus all the surfaces of components are exposed to the cooling fluid. Kim and Anand [3] simulated heat transfer between a series of parallel plates with surface-mounted discrete heat

* Corresponding author, e-mail: vadimd@bgu.ac.il

sources. The numerical simulation and implementation of k-ε model was validated by comparing with published experimental data. Davalath and Bayazitoglu [4] numerically studied forced convection between parallel plates mounted with 2-D multiple blocks. Results indicated that the heat flux distributions at the rear surfaces of blocks are much smaller than those at the front and top surfaces. Asako and Faghri [5] performed a 3-D analysis for heat transfer and flow through an array of heated square blocks. Their results illustrated that the local heat flux on the top surface of block is higher than those on the front, side and rear surfaces.

Chen and Wang [6] investigated numerically and experimentally the turbulent forced convective flow over a heated block mounted on an adiabatic wall for different Reynolds number and the aspect ratio of the block. Jacobi and Shan [7] demonstrated the features of flow passing a rectangular step: boundary-layer separation, reattachment, and growth are shown. A free-shear layer is also identified. Wong and Peck [8] performed an experiment to investigate the effect of altitude on the characteristic of heat transfer from blocks to air stream. Sara *et al.* [9] experimentally studied enhancement of heat transfer from a flat surface in a channel by attachment to rectangular cross-sectional blocks as a function of the flow and geometrical parameters. The net effect of the blocks on the heat transfer is governed by two factors: the increase in the heat transfer surface area and the disturbances in the flow. Ryu *et al.* [10] indicated that the different block arrangements exhibit distinct flow characteristics and heat transfer that were higher than those of the flat surface. Tsay and Cheng [11] numerically investigated the 2-D forced convection in a channel containing short multi-boards mounted with heat generating rectangular blocks. The ratio of spacing between blocks, to block height from 5 to 30 was studied. Owing to the effects of thermal interactions among the sub-streams of fluid through the conducting boards, the deviation in heat transfer characteristics of the blocks mounted on different board was rather substantial. Heat transfer increased with increasing block height. An experiment has been carried out by Nakamura and Igarashi [12] to investigate the forced convection heat transfer from a low-profile block, 2 mm high, placed in a rectangular duct, 3.8-10 mm wide, with mean duct velocity upstream of the block, which ranged from 0.24 to 4 m/s.

Research in this area is currently intensively continued. Yemenici and Umur [13] experimentally investigate heat transfer enhancement over a flat, concave, convex, and ribbed surfaces encompassing laminar, transitional, and turbulent flows. The ribbed surface with the same heated area caused most of the heat transfer augmentation above the flat surface: 160% in laminar flows and 120% in turbulent flows. Buyruk and Karabulut [14] numerically evaluated the potential of different types of rectangular fins of different heights and angles. Srinivasan *et al.* [15] studied heat transfer characteristics of a high aspect ratio channel featuring ribs and trenches. The presence of ribs yielded higher enhancement levels in comparison to the trenches.

In our current work we study plates with rectangular hollow blocks of a square form, having equal vertical and horizontal extension sizes. A typical profile is shown in fig. 1. Plates are placed in the center of a narrow channel with their two-sided heat transfer to air in forced convection. In such constructions, obviously, the heat flux to air in any cross-section at both sides is significantly different.

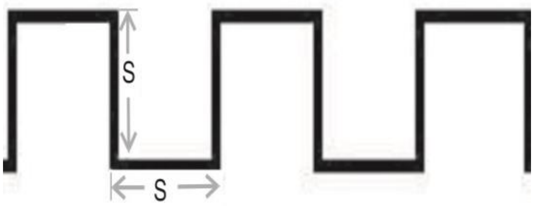

Figure 1. Profile of studied plates

Experimental set-up and numerical procedure

Experimental set-up

Experimental set-up was based on four electrically heated plates, fig. 2. Four plates, Z = 30 mm wide and L = 260 mm of length were considered. Three plates were extended perpendicular to air-flow by square profile of fig. 1. The first one with six rectangular extensions, 10 × 10 mm (n_s = 6, S = 0.01 m), the next one with nine rectangular extensions 6 × 6 mm (n_s = 9, S = 0.006 m), and the other one with eighteen rectangular extensions 3 × 3 mm (n_s = 18, S = 0.003 m). The fourth one was used as a flat plate. So, an unfolded length of all plates was the same, while the real length of extended part of three extended plates were about 120 mm. All plates were placed in the center of a rectangular channel of 45 × 20 mm (Z_{ch} = 0.045 m, W = 0.02 m) cross-section. Electric heating was carried out at a power of 5-10 W (700-1400 W/m^2). Experimentally investigated range of air superficial velocities was from 1 to 3 m/s. In general, the studied range of Reynolds numbers related to the free part of channel was from 1200 to 5000. Temperature was measured on the heated plate (5 points), and of the cooling air (4 points), which were used for the average temperatures calculations of heated plates and air.

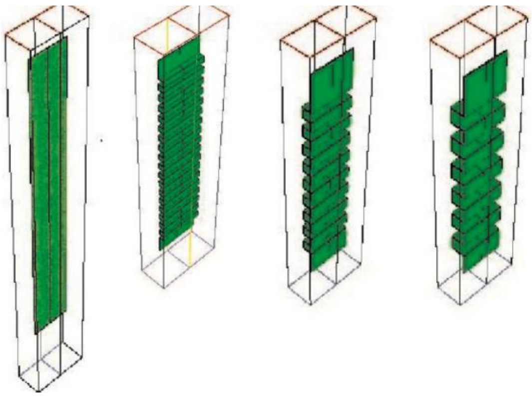

Figure 2. Experimental plates

The experiments were repeated twice: for unpainted plates with minimum heat radiation and for the painted in black color, with a maximum heat radiation. These datas were compared with numerical calculations using emissivity 0 and 1, respectively. The surface temperatures were recorded by an infrared camera, focused on the plate surfaces. In accordance with the specifics of the camera, temperature recordings were made for painted in black color plates.

Numerical procedure

For the computational procedure, the structure was divided by vertical plane of symmetry. This division yielded a half of the original space, defined as the 3-D computational domain with preset temperature, air velocity at the inlet and pressure at the outlet. The heated plates were modeled similarly as they were built in reality, as a heat-generating source, while its entire volume was represented by a *conducting wall*. The numerical computations were performed for the steady-state velocity and temperature fields in air and temperature fields on the plates. The basic conservation equations were solved for the 3-D system, using the FLUENT 6.3 CFD software. The Boussinesq approximation was not used, and the density-temperature, viscosity-temperature, and conductivity-temperature relations were provided as an input for forced flow. Flat plate calculations were carried out by using the laminar model. For the extended plate cases the k-ε turbulent model was used. For the experimentally studied plates calculations were repeated twice: with and without heat radiation and compared to the corresponding experiments, as mentioned above. Heat radiation is computed by applying DTRM model.

The computational grid was formed uneven. The cells were formed as hexahedral cells of size 0.33-0.5 mm having a total amount of 1040000 elements for a flat plate, 2200000 for the extended 3 mm plate, 2000000 for the extended 6mm plate, and about 2350000 elements for the extended 10 mm plate.

Also numerical analysis of the plate height-to-width ratio was carried out.

Validation

Grid refinement

The refinement of the grid was carried out by calculating some individual typical modes by the same model with elements of smaller size, while the total number of elements increased by more than 50%. Thus, for a control calculation of the extended 10 mm plate, the total number of elements exceeded 4 million. These calculations did not show any significant effect.

Effect of heat radiation on the convective heat transfer coefficient

A large number of calculations were performed taking into account the radiation for comparison with the experiments. In parallel, these regimes were calculated without radiation. Naturally, other temperature fields were obtained. Comparison of the average convective heat transfer coefficient showed a slight difference in results, less than 4%. This corresponds to the average temperatures differences, and considerably exceeds the accuracy of the experimental data.

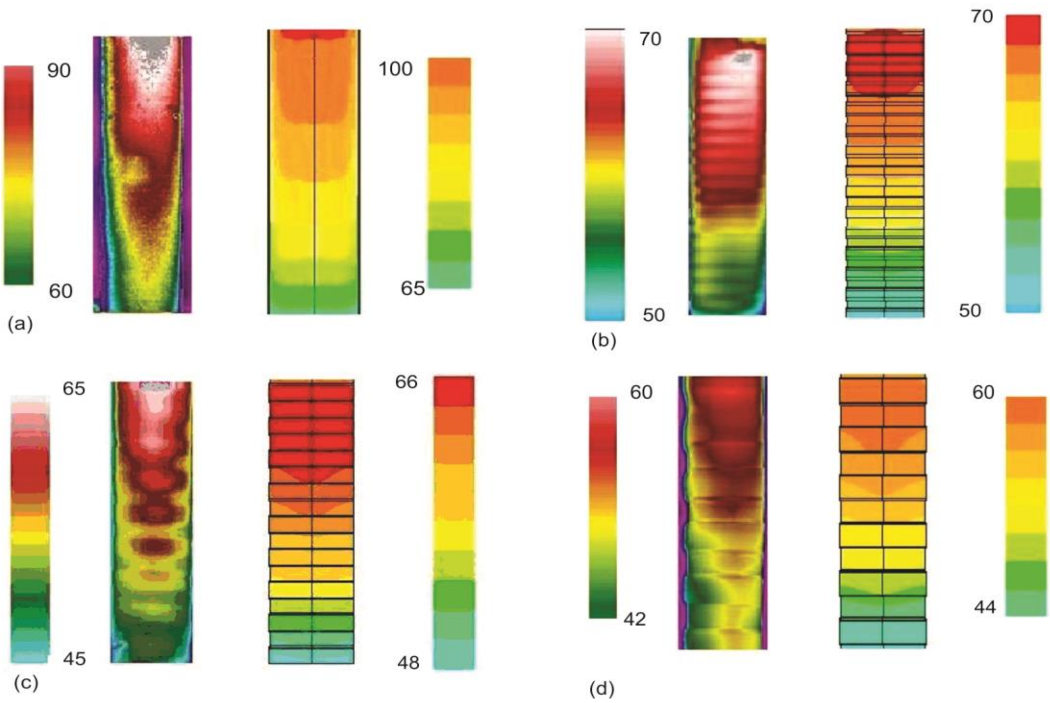

Figure 3. Surface temperatures, [°C]: experimental infrared camera recording, and the results of FLUENT calculations: q'' = 1400 W/m^2, V_{air} = 3 m/s; (a) flat plate, (b) extended 3 mm plate, (c) extended 6 mm plate, and (d) extended 10 mm plate (*for colour image see journal web site*)

Experimental data and comparison to numerical results

Experimental temperatures of surfaces recorded by the infrared camera, and calculated temperature fields are shown in fig. 3. Infrared temperature recordings for painted in black color plates (left sides) were compared with calculations (right sides) taking into account radiation heat transfer. A case of forced convection at 3 m/s air velocity and maximum heating for all four heated plates is presented.

Figure 4 shows a comparison of the heat transfer parameters (Nu-Re relations) obtained from the experimental data on unpainted plates, with numerical calculations in the absence of radiation. The average heat transfer coefficient was defined through the difference between the average temperatures of both the heated plate and flowing air in the channel. Reynolds number and Nusselt number were based on average values of thermal conductivity, viscosity, average heat flux, temperature difference between average plates and air temperatures, both for processing experimental and numerical data.

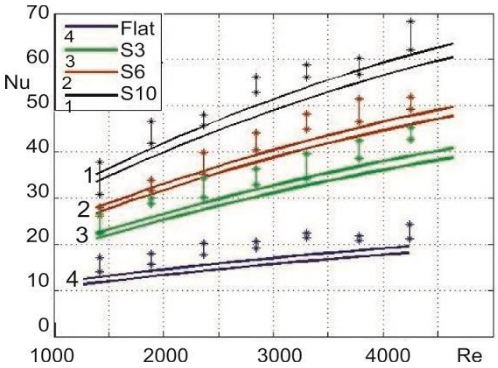

Figure 4. Heat transfer without radiation: experiments and numerical calculations

As previously mentioned, the superficial air velocities in the channel were used. The hydraulic diameter, *d*, was adopted as a linear dimension.

Correspondingly, comparison of experiments of painted in black color plates, and calculations taking into account radiation are shown in fig. 5.

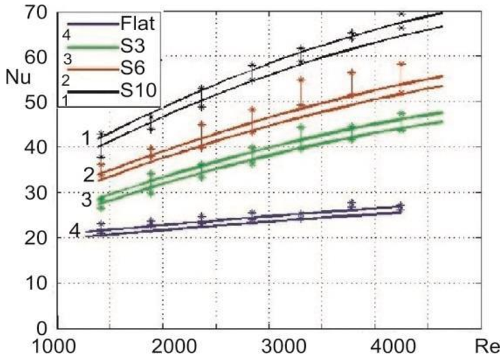

Figure 5. Heat transfer with radiation: experiments and numerical calculations

Main comparison of numerical calculations and the processing of experimental data have demonstrated the following results:

– The experimental and calculated data showed a significant increase in heat transfer coefficient for extended plates as compared to the flat plate. That increase was growing rapidly with increasing air velocity.

– The experimental and calculated data showed somewhat higher heat transfer coefficient of the plate with larger extensions.

– The difference between the experimental and calculated data of unpainted flat plate in fig. 4 indicates that radiation takes place for the unpainted plates, too, with a substantially non-zero emissivity, in contrast to the calculation without radiation.

– In general, the results show a good qualitative and satisfactory quantitative agreement between the numerical calculations and the experimental data.

General numerical results and discussion

As already mentioned, the aim of current work is to analyze and compare the average characteristics of the heat transfer processes for the considered cases of heated plates cooled in an air-flow in narrow channels. Thus, the local values of heat transfer coefficients were not investigated.

Correlations for the flat heated plate

Following the experiments, calculations were made for air velocities from 0.3 m/s to 3 m/s. The range of heat flux varied from 700 to 2000 W/m^2. Further, constructive variations were studied. First, the plate length was reduced and analyzed. Secondly, for the original length, the width of the plate was increased and analyzed in such a way that it reached a square form. In this case the width of the channel also increased proportionally, to preserve the ratio of the width of the channel to be 50% larger than the plate width. In addition, for a square plate, calculations were made for a narrower channel, 10 mm thick.

The well-known relations for laminar heat transfer in tubes were used, eq. (1), is the eqs. (6)-(10) in Holman, [16], where constant C = 1.86:

$$\mathrm{Nu} = C\left(\mathrm{Re}\,\mathrm{Pr}\right)^{1/3}\left(\frac{d}{L}\right)^{1/3}\left(\frac{\mu}{\mu_{\omega}}\right)^{0.14} \tag{1}$$

We have followed and processed our results in the same manner and we obtained similar results, but with a coefficient 2.77 instead of 1.86. Very good agreement has been achieved as shown in fig. 6.

Thus, laminar heat transfer over a heated flat plate located in the center of a narrow channel is represented by eq. (1) with C = 2.77. This relates to the channel width 50% larger than the width of the flat plate.

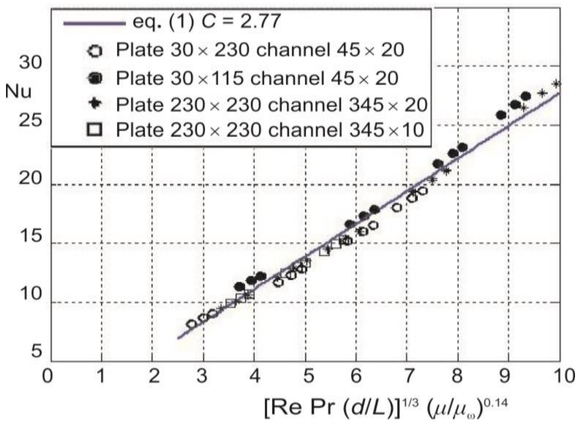

Figure 6. Heat transfer correlations for flat plate

Heat transfer for extended plates in a narrow channel

The temperature and the heat flux distribution on the plate, air temperature and velocity, for the extended 10 mm plate without radiation are shown in figs. 7-9, illustrating the mode selected, having the maximum heat input and the maximum air velocity.

In fig. 7 was imposed left-right symmetry about vertical symmetry cross-section. In figs. 8 and 9 air temperatures and air velocities were shown at different vertical cross-sections (left to right): symmetry; 7.5 mm from symmetry (center of the plate half); 15 mm from symmetry (edge of plate); 19mm from symmetry (center of free channel).

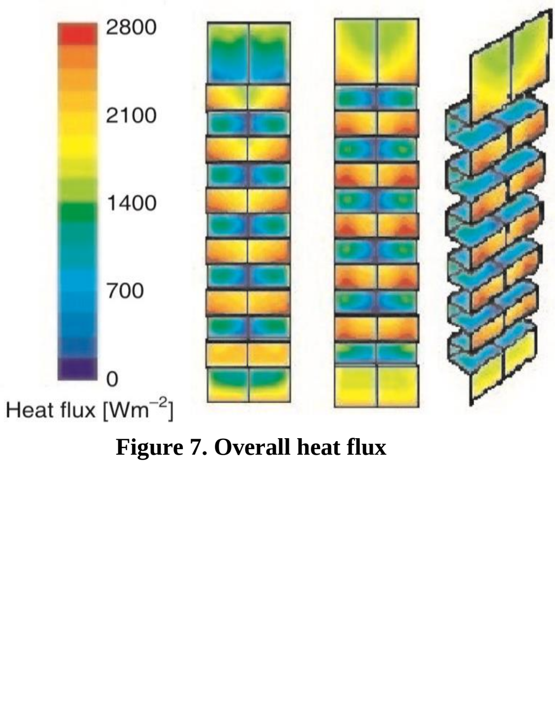

Figure 7. Overall heat flux

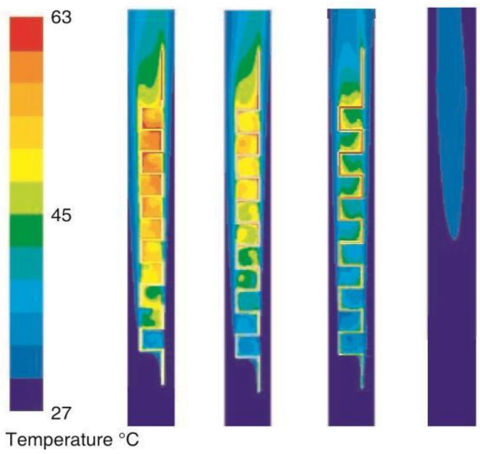

Figure 8. Air temperature in different cross-sections

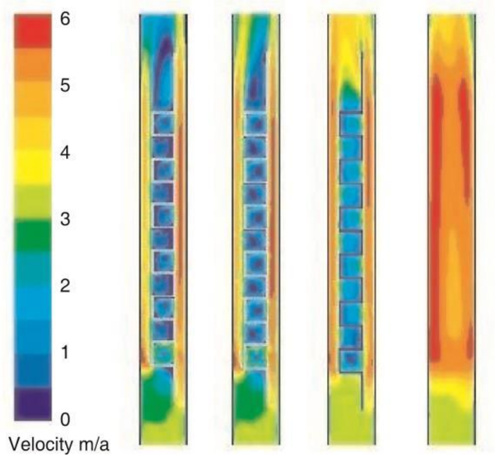

Figure 9. Air velocities in different cross-sections

Overall heat transfer correlation for extended plates

For the extended plates in addition to the basic construction, were also considered plates of larger width, which was approximately equal to the height of the active part. So, the active part had a square shape (width about 120 mm).

The results have illustrated that in our case the Nusselt number relates to Reynolds number to the power of 0.5, at which the results for each extension are very well linearzed.

Correspondingly, the correlations for different extensions have the following form:

$$\mathrm{Nu} = C_1 \,\mathrm{Re}^{0.5}\,\mathrm{Pr}^{1/3}\left(\frac{\mu}{\mu_\omega}\right)^{0.14} \tag{2}$$

The constant C_1 for various extension values is given in tab. 1.

Table 1. Values of constant C_1

Extension size, S	10 mm	6 mm	3 mm
Constant, C_1	1.01	0.81	0.63

Additional calculations were carried out changing the thickness of the channel, in the following range: the extension sizes, S, were from 1 to 15 mm, the thickness of the channel, W, was from 6.7 to 33 mm, the ratio of the extension to the thickness, S/W, was from 0.15 to 0.5. These calculations confirmed the correlation of the Nusselt number with respect to the ratio of S/W raised to the power of 0.4. The effect of an increase in the channel width up to 60 mm was investigated while maintaining the plate width at 30 mm (ratio Z_{ch}/Z was increased from 1.5 to 2). A relation was obtained for the Nusselt number to the same power of 0.4. Accordingly, the general relation for all extended plates took the form of eq. (3), as shown in fig. 10:

$$\mathrm{Nu} = 1.556\left(\frac{S}{W}\frac{Z}{Z_{\mathrm{ch}}}\right)^{0.4}\mathrm{Re}^{0.5}\,\mathrm{Pr}^{1/3}\left(\frac{\mu}{\mu_\omega}\right)^{0.14} \tag{3}$$

Relation between fluid pressure losses and heat transfer for extended plates

In the calculations the assumption was that the pressure losses in the channel are mainly losses on the rectangular extensions only and are evenly distributed on the plate. Therefore, the processing of the results is carried out with respect to the loss coefficient f_s, defined by eq. (4), where Δp is the total pressure loss in the channel, and n_s is the number of rectangular extensions:

$$\Delta p = n_s f_s \rho \frac{V_{\mathrm{air}}^2}{2} \tag{4}$$

The processing of the results made it possible to linearize the dependence of the loss coefficient, f_s, on the complex $\mathrm{Re}^{-0.5}(S/W)^2$ as shown in fig. 11 (for $Z_{\mathrm{ch}}/Z = 1.5$). Accordingly, the relation has the form of eq. (5):

$$f_s = 38\,\mathrm{Re}^{-0.5}\left(\frac{S}{W}\right)^2 \tag{5}$$

For a plate of length, L, the coefficient is multiplied by the number of rectangular extensions, n_s. If L is used as the real length of the extended plate, then $n_s = (L/2S)$. If L is an unfolded length, then $n_s = (L/4S)$. For the length L as the real plate length:

$$f_L = f_s\left(\frac{L}{2S}\right) = 19\,\mathrm{Re}^{-0.5}\left(\frac{S}{W}\right)\left(\frac{L}{W}\right) \tag{6}$$

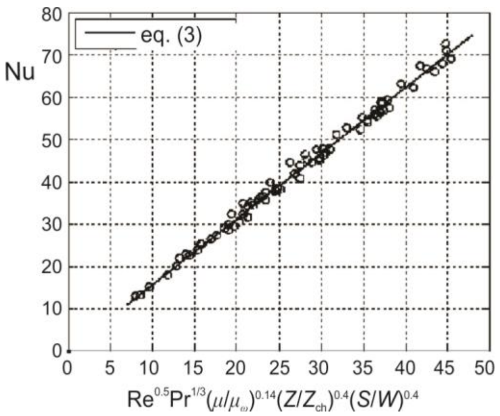

Figure 10. Overall heat transfer correlations for extended plates

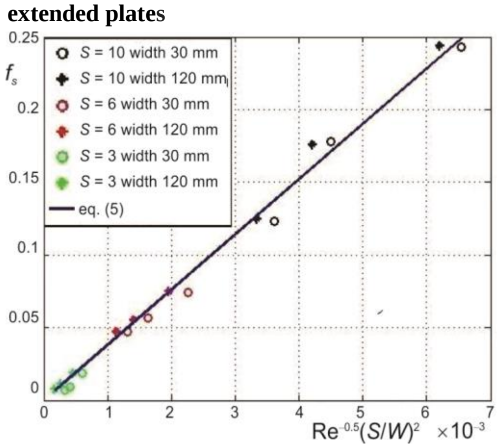

Figure 11. Correlation for pressure losses coefficient defined by eq. (5) for one square extension

The ratio of the heat transfer rate to the pressure losses is of interest. Combining eqs. (3) and (6), neglecting the change in viscosity we obtain in terms of the Stanton number:

$$\frac{\mathrm{St}\,\mathrm{Pr}^{2/3}}{f_L} = 0.07\left(\frac{W}{S}\right)^{0.6}\left(\frac{W}{L}\right) \tag{7}$$

If L is assumed as an unfolded plate length, then the coefficient in eq. (7) is 0.14 instead of 0.07. This heat rate – pressure losses relation for air-flow in a narrow channel with rectangular extended heated plates closely resembles that for tube flow. Indeed, in eqs. (6)-(12) for a tube flow (Holman [16]), and in our eq. (7) the left-hand sides coincide.

Summary

Numerical and experimental study of heat transfer enhancement on heated extended plates inserted in narrow rectangular channels and cooled in air forced convection has been presented.

The generalization of the performed numerical calculations made it possible to obtain the relation of heat transfer as a function of the extension size. For this purpose, calculations were made for the entire range of extension sizes from 1 mm to 15 mm. Correlation was also obtained for a flat plate placed in this channel.

For three extension sizes (3, 6, and 10 mm), as well as for a flat plate, experiments were carried out. That made it possible to compare both the average characteristics of heat transfer to air, and the temperature fields on plates by using the infrared camera, focused on the plate's surfaces. The experimental results and the numerical calculations showed quantitatively a satisfactory agreement.

A numerical analysis of the ratio of plate height to width and channel sizes was also carried out and yielded a generalized correlation.

Both the experimental and calculated data showed a significant enhancement of heat transfer for the extended plates *vs*. flat plate. Somewhat higher heat transfer rate was obtained for larger extension sizes.

Relation between fluid pressure losses and heat transfer rates was studied and generalized.

Nomenclature

C, C_1 – constants, [–]
d – channel hydraulic diameter, [m], [mm]
f_L – pressure loss coefficient of channel, [–]
f_s – pressure loss coefficient of one extension, [–]
h – heat transfer coefficient, [$\mathrm{Wm^{-2}K^{-1}}$]
k – air thermal conductivity, [$\mathrm{Wm^{-1}K^{-1}}$]
L – plate length, [m], [mm]
Nu – Nusselt number, (= hd/k)
n_s – blocks (extensions): number of them, [–]
Pr – Prandtle number
Δp – pressure loss, [Pa]
q'' – heat flux, [$\mathrm{Wm^{-2}}$]
Re – Reynolds number, (= $V_{\mathrm{air}}d\rho/\mu$)
S – block (extension) size, [m], [mm]
St – Stanton number, (= Nu/RePr)
V_{air} – air velocity, [$\mathrm{ms^{-1}}$]
W – channel thickness, [m], [mm]
Z_{ch} – channel width, [m], [mm]
Z – plate width, [m], [mm]

Greek symbols

μ – air viscosity dynamic, [$\mathrm{kgm^{-1}s^{-1}}$]
μ_ω – air viscosity dynamic at wall, [$\mathrm{kgm^{-1}s^{-1}}$]
ρ – air density, [$\mathrm{kgm^{-3}}$]

References

[1] Sparrow, E. M., *et al*., Heat Transfer and Pressure Drop Characteristics of Arrays of Rectangular Modules Encountered in Electronic Equipment, *Int. J. Heat and Mass Transfer*, *25* (1982), 7, pp. 961-973
[2] Chang, W. J., You, Y. D., Hot Block Elevation Effect on Mixed Convection in a Parallel Plate Channel, *Numer. Heat Transfer*, 29 (1996), Part A, pp. 297-312
[3] Kim, S. H., Anand, N. K., Turbulent Heat Transfer Between a Series of Parallel Plates with Surface-Mounted Discrete Heat Sources, *ASME J. Heat Transfer*, *116* (1994), 3, pp. 577-587
[4] Davalath, J., Bayazitoglu, Y., Forced Convection Cooling Across Rectangular Blocks, *ASME J. Heat Transfer, 109*, (1987), 2, pp. 321-328
[5] Asako, Y., Faghri, M., Three-Dimensional Heat Transfer Analysis of Arrays of Heated Square Blocks, *Int. J. of Heat and Mass Transfer, 32* (1989), 2, pp. 395-405
[6] Chen, Y. M., Wang, K. C., Simulation and Measurement of Turbulent Heat Transfer in a Channel with a Surface-Mounted Rectangular Heated Block, *Heat Mass Transfer, 31* (1996), 6, pp. 463-473
[7] Jacobi, A. M., Shan, R. K., Air-Side Flow and Heat Transfer in Compact Heat Exchangers: A Discussion of Enhancement Mechanisms, *Heat Transfer Engineering, 19* (1998), 4, pp. 29-41
[8] Wong, H., Peck, R. E., Experimental Evaluation of Air-Cooling Electronics at High Altitudes, *ASME J. Electron. Packaging, 123* (2001), 4, pp. 357-365
[9] Sara, O.N., *et al*., Enhancement of Heat Transfer From a Flat Surface in a Channel Flow by Attachment of Rectangular Blocks, *Int. J. of Energy Research, 25* (2001), 7, pp. 563-576

[10] Ryu, D. N., *et al*., Analysis of Turbulent Flow in Channels Roughened by 2-D Ribs and 3-D Blocks, Part II: Heat Transfer, *Int. J. of Heat and Fluid Flow, 28* (2007), 5, pp. 1112-1124
[11] Tsay, Y. L., Cheng, J. C., Analysis of Convective Heat Transfer Characteristics for a Channel Containing Short Multi-Boards Mounted with Heat Generating Blocks, *Int. J. of Heat and Mass Transfer, 51* (2008), 1-2, pp. 145-154
[12] Nakamura, H., Igarashi, T., Forced Convection Heat Transfer from a Low-Profile Block Simulating a Package of Electronic Equipment, *ASME J. Heat Transfer 126* (2004), 3, pp. 463-470
[13] Yemenici, O., Umur, H., Experimental Aspects of Heat Transfer Enhancement over Various Flow Surfaces, *Heat Transfer Engineering, 37* (2016), 5, pp. 435-442
[14] Buyruk, E., Karabulut, K., Enhancement of Heat Transfer for Plate Fin Heat Exchangers Considering the Effects of Fin Arrangements, *Heat Transfer Engineering, 39* (2018), 15, pp. 1392-1404
[15] Srinivasan, S., *et al*., Heat Transfer Measurements inside Narrow Channels with Ribs and Trenches, *Heat Transfer Engineering, 39* (2018), 9, pp. 750-759
[16] Holman, J., *Heat Transfer*, 10^{th} edition, McGraw-Hill, New York, USA, 2010

Paper submitted: January 12, 2019
Paper revised: February 26, 2019
Paper accepted: April 8, 2019